TECHNICAL ARTICLE

Reflection splitting-induced microstrain broadening

Andreas Leineweber[a)]
Institute of Materials Science, Gustav-Zeuner-Straße 5, TU Bergakademie Freiberg, 09599 Freiberg, Germany

(Received 29 August 2016; accepted 11 May 2017)

Crystal structure determination on the basis of powder diffraction data frequently involves the question how the given diffraction data with some appreciably *hkl*-dependent line broadening should be interpreted. In many cases, such line broadening may either: (i) reasonably well be reconciled with a certain high-symmetry structure model or (ii) with a variant of the former with lower symmetry crystal family, which frequently will give a somewhat better fit in Rietveld refinement. In this work, it is shown mathematically that symmetry reduction induced reflection spitting masked by other line broadening contributions, thus leading to some reflection splitting-induced line broadening, shows a similar *hkl* dependence as typically adopted for anisotropic microstrain broadening with respect to the high-symmetry structure. This implies that Rietveld refinement on the basis of the low-symmetry model (including typically isotropic line broadening) and on the basis of the high-symmetry model with anisotropic microstrain broadening can both lead to similar qualities of the fit. Hence, the refinement results for both possibilities should be carefully considered in combination with possibly available additional information (e.g. results of first-principles calculations) to arrive at adequate conclusions concerning the true symmetry of the material under investigation. © *2017 International Centre for Diffraction Data*. [doi:10.1017/S0885715617000665]

Key words: line broadening analysis, symmetry reduction, strain, microstrain

I. INTRODUCTION

Many phase transitions from a high-symmetry to a low-symmetry phase show up in powder diffraction patterns by a splitting of reflections, which are equivalent and occur at the same diffraction angle for the high-symmetry phase. Such a splitting can occur if the symmetry reduction involves reduction of the symmetry of the crystal family. Thereby, the phase transition is connected with a strain, which itself breaks the symmetry of the high-symmetry phase.

In the course of such phase transition, a crystal of the high-symmetry phase may split up into many low-symmetry phase domains. Generally, these domains can be classified as belonging to a finite number of *domain states* (Janovec and Privratska, 2003). This number corresponds to the ratio of the orders of the space groups of high- and low-symmetry phase. If the phase transformation involves occurrence of symmetry-breaking strain, all or groups of the domain states are characterized by different orientations of the strain tensor. In what is sometimes called *pure ferroelastics*, all domain states feature differently oriented strain. If the phase transitions also involve formation of chiral, ferroelastic, and/or antiphase domains, there will be groups of domain states of the same orientation of the strain. These groups will, however, deal with here as a whole, as only the strains are of interest.

In particular, the presence of domain (twin) boundaries separating domains of different strains can lead to peculiar diffraction phenomena, which may more or less strongly influence the regions of splitting fundamental reflections in powder diffraction patterns (Cowley and Au, 1978; Hayward and Salje, 2005; Boysen, 2007; Leineweber, 2012a; Leineweber and Krumeich, 2013), whereby occurrence of interference between X-rays/neutron scattered in differently oriented domains is particularly complex phenomenon. These peculiar interference phenomena will, however, not be considered in the present paper. Instead, in the present paper, the case is investigated more closely, where the spontaneous symmetry-breaking strain leads for the low-symmetry phase to an only very small reflection splitting in powder diffraction patterns, the shape of which then gets masked by other, e.g. instrumental line broadening contributions. Therefore, the reflection splitting shows mainly up as some line broadening, which can easily be mixed up with ordinary line broadening of the high-symmetry phase. This apparent line broadening has very similar properties as the *hkl*-dependent microstrain broadening commonly applied in Rietveld refinement.

II. CONCEPTS USED

A. Symmetry-breaking spontaneous strain

In order to be able to analyze the line broadening effects because of reflection splitting in the following sections, a treatment of symmetry-breaking strain according to Aizu (1970) introduced in the context of analysis of ferroelastic phase transitions will be adapted for the present purposes. Aizu, in particular, dealt with the problem that, in the existence regime of a low-symmetry (often low-temperature) phase, frequently the high-symmetry phase is not stable and cannot be studied. This obstructs precise determination of the strain describing the distortion of the low-symmetry phase with respect to the high-symmetry phase at a specific temperature and pressure,

a)Author to whom correspondence should be addressed. Electronic mail: andreas.leineweber@iww.tu-freiberg.de

which is needed for detailed analysis of strains, e.g. by means of Landau theory (Carpenter *et al.*, 1998). Aizu proposed to refer the strain associated with the low-symmetry state relative to some specific hypothetical high-symmetry state, which has a lattice metric purely derived from the metric of the low-temperature state. For that Aizu required the sum over the strain tensors ${}^m\boldsymbol{\varepsilon}_S$ pertaining to the n different domain states amounts 0:

$$\sum_{m=1}^{n} {}^m\boldsymbol{\varepsilon}_s = 0 \tag{1}$$

whereby the tensors had originally been denoted as x_s by Aizu (1970). Equation (1) implies that the metric of the high-symmetry phase is some averaged metric of the low-symmetry phase. Note, moreover, that because of their definition, the tensors ${}^m\boldsymbol{\varepsilon}$ have a trace of 0. Note, moreover, that the n tensors ${}^m\boldsymbol{\varepsilon}_s$ are inter-related with each other by tensor transformations using the symmetry operators $\boldsymbol{R}$, which get lost upon reducing the symmetry from the high- to the low-symmetry phase:

$$\boldsymbol{R}\,{}^m\boldsymbol{\varepsilon}_s\boldsymbol{R}^T = {}^{m'}\boldsymbol{\varepsilon}_s \tag{2}$$

In order to quantify the symmetry-breaking strain exerted by ${}^m\boldsymbol{\varepsilon}_s$, Aizu (1970) suggested use of a scalar magnitude ε_s called the *spontaneous strain* ε_s (originally called x_s) defined as

$$\begin{aligned}\varepsilon_s^2 = \sum_{i,j=1}^{3} {}^m\varepsilon_{sij}^2 &= {}^m\varepsilon_{s11}^2 + {}^m\varepsilon_{s22}^2 + {}^m\varepsilon_{s33}^2 \\ &+ 2{}^m\varepsilon_{s12}^2 + 2{}^m\varepsilon_{s13}^2 + 2{}^m\varepsilon_{s23}^2\end{aligned} \tag{3}$$

ε_s does not change upon transformation of ${}^m\boldsymbol{\varepsilon}_s$, which means that its value is independent of m.

Aizu indicated that the (then ferroelastic) symmetry distortion increases upon increase of ε_s. A more explicit meaning of the value of ε_s can be derived by analyzing how ε_s is related with the variation of the strain ${}^m\boldsymbol{\varepsilon}_s(\boldsymbol{x})$ measured along a unit vector $\boldsymbol{x}$ in the crystal frame of reference:

$${}^m\varepsilon_s(\boldsymbol{x}) = {}^m\varepsilon_{sij}x_ix_j \tag{4}$$

applying here and henceforth the Einstein summation convention. The direction average of this and other scalar quantities can be obtained by expressing the components of $\boldsymbol{x}$ in polar coordinates ($x_1 = \cos\varphi\sin\vartheta$, $x_2 = \sin\varphi\sin\vartheta$, $x_3 = \cos\vartheta$) and integrating over $\sin\vartheta/(4\pi)d\vartheta d\varphi$ from 0 to π for ϑ and 0 to 2π for φ. Equation (4) yields after integration

$$\begin{aligned}\bar{\varepsilon} &= \frac{1}{4\pi}\int_0^{2\pi}\int_0^{\pi} {}^m\varepsilon_{sij}x_ix_j \sin\vartheta d\vartheta d\varphi \\ &= \tfrac{1}{3}({}^m\varepsilon_{s11} + {}^m\varepsilon_{s22} + {}^m\varepsilon_{s33})\end{aligned} \tag{5}$$

Equation (5) is, like Eq. (3), invariant with respect to tensor transformation of ${}^m\boldsymbol{\varepsilon}_s$ and is, therefore, m-independent and amounts 0 in line with the definition of this strain tensor (see above). Note that, here and henceforth, the overbar will be used to indicate an average over all directions of $\boldsymbol{x}$ (see Leineweber, 2016). The anisotropy of the direction-dependent strain can be quantified by its variance, $\overline{(\varepsilon - \bar{\varepsilon})^2} = \overline{\varepsilon^2}$, which then is obtained in view of Eq. (5) as

$$\begin{aligned}\overline{(\varepsilon - \bar{\varepsilon})^2} = \overline{\varepsilon^2} &= \frac{1}{4\pi}\int_0^{2\pi}\int_0^{\pi} \left({}^m\varepsilon_{sij}x_ix_j\right)^2 \sin\vartheta d\vartheta d\varphi, \\ &= \frac{1}{15}\left(3{}^m\varepsilon_{s11}^2 + 3{}^m\varepsilon_{s22}^2 + 3{}^m\varepsilon_{s33}^2 + 2{}^m\varepsilon_{s11}{}^m\varepsilon_{s22}\right. \\ &\quad + 2{}^m\varepsilon_{s11}{}^m\varepsilon_{s33} + 2{}^m\varepsilon_{s22}{}^m\varepsilon_{s33} \\ &\quad \left. + 4{}^m\varepsilon_{s12}^2 + 4{}^m\varepsilon_{s13}^2 + 4{}^m\varepsilon_{s23}^2\right)\end{aligned} \tag{6a}$$

whereby the upper left index of m is omitted for the variances because the result is, again, m-independent.

Subtraction of $0 = 1/15({}^m\varepsilon_{s11} + {}^m\varepsilon_{s22} + {}^m\varepsilon_{s33})^2$ from Eq. (6a) gives

$$\overline{\varepsilon^2} = \frac{2}{15}\left({}^m\varepsilon_{s11}^2 + {}^m\varepsilon_{s22}^2 + {}^m\varepsilon_{s33}^2 + 2{}^m\varepsilon_{s12}^2 + 2{}^m\varepsilon_{s13}^2 + 2{}^m\varepsilon_{s23}^2\right) \tag{6b}$$

which is again independent of m. Comparison of Eq. (6b) with Eq. (3) shows, that the spontaneous strain ε_S introduced by Aizu (1970) is proportional to the variance of the direction-dependent strain caused by ${}^m\boldsymbol{\varepsilon}_s$.

B. General description of microstrain broadening

Microstrain in an untextured crystalline material implies, in the crystal frame of direction, a distribution of strain around its average, defined as strain $\langle\boldsymbol{\varepsilon}\rangle = 0$ in the present work. At this zero strain, the material exhibits its average lattice parameters. The microstrain can then be understood as a correlated distribution of the components of the strain tensor $\boldsymbol{\varepsilon}$ around zero strain. That distribution is usually regarded as unimodal, and if it is symmetric, it has its maximum at $\langle\boldsymbol{\varepsilon}\rangle = 0$. Typical origin of such microstrain is sufficiently long-range distortions of the crystal lattice (i.e. strains) randomly occurring over the diffracting material because of some microstructural inhomogeneities, like composition variations, temperature variations, and, most prominently, locally varying stresses (microstress) caused by dislocations but also by pure elastically accommodated misfit between grains within a polycrystal.

By means of powder diffraction, this microstrain can be characterized by analyzing the microstrain measured in the direction of reciprocal lattice vectors (i.e. the broadening for different *hkl*) and making conclusions about the overall microstrain distribution).

The correlated distribution of the components of the strain tensor around their average values is conveniently done by means of the tensors quantifying the joint central moments (or cumulants) of second and higher order (Leineweber, 2009, 2011). In most cases, only the second moments are considered, i.e. the variances and covariances of the strain tensor's components, which are (for averages = 0) given as the at maximum 81 components $E_{ijpq} = \langle\varepsilon_{ij}\varepsilon_{pq}\rangle$ of a fourth rank tensor $\boldsymbol{E}$. At maximum 21 of these components are independent; that number can be further reduced by crystal symmetry. The variance of the microstrain broadening measurable in a direction $\boldsymbol{x}$ is

https://doi.org/10.1017/S0885715617000665 Published online by Cambridge University Press

then given by the polynomial

$$\langle \varepsilon_{hkl}^2 \rangle = \langle \varepsilon^2(x) \rangle = \langle \varepsilon_{ij} \varepsilon_{pq} \rangle x_i x_j x_p x_q \quad (7)$$

Thereby, the *hkl* dependence of $\langle \varepsilon_{hkl}^2 \rangle = \langle \varepsilon^2(\boldsymbol{x}) \rangle$ is contained in the components of x_1, x_2, and x_3, which are linearly related with h, k, and l. Note that now the $\langle\rangle$ indicates averaging over the different strain values over the ensemble of crystallites/domains, now not involving direction averaging indicated by the overbar (see above). In the course of Rietveld refinement, $\langle \varepsilon_{hkl}^2 \rangle$ is typically associated with a certain shape for the line broadening, most frequently with a Gaussian. (In the case that the line broadening is/appears to be of Lorentzian or pseudo-Voigt shape (Stephens, 1999), alternative width parameters have to be used, since the variance does not exist for these shapes, as long as the pseudo-Voigt does not correspond to a pure Gaussian. See also Leineweber (2011).) Thereby, fitting on the basis of experimental data is done with only 15 independent fitting parameters, the number of which can be further reduced by the crystal symmetry, which are given by

$$Z_{ijpq} = \tfrac{1}{3}\left(\langle \varepsilon_{ij} \varepsilon_{pq} \rangle + \langle \varepsilon_{ip} \varepsilon_{jq} \rangle + \langle \varepsilon_{iq} \varepsilon_{jp} \rangle \right) \quad (8)$$

These Z_{ijpq} parameters can be used to analyze the above mentioned microstructural characteristics provided that a model exists relating strain and inhomogeneously distributed quantities causing the microstrain (composition, temperature, stress).

III. REFLECTION SPLITTING-INDUCED MICROSTRAIN BROADENING

Upon reducing the symmetry of the crystal family of a high-symmetry structure, the accompanying symmetry-breaking strain will, in a powder-diffraction pattern, lead to some reflection splitting for some or all *hkl* pertaining to the high-symmetry phase. This is because of a probability density function of strain along the diffraction vector, which is a superposition of n delta functions located at the values ${}^m\boldsymbol{\varepsilon}_s(\boldsymbol{x})$ according to Eq. (4) with $m = 1 \ldots n$, where $\boldsymbol{x}$ is the unit vector parallel to the diffraction vector of any of the *hkl* reflections of the high-symmetry structure. Averaging over these strain values yields with use of Eq. (1):

$$\langle \varepsilon \rangle(x) = \frac{1}{n} \sum_{m=1}^{n} \left({}^m\varepsilon_{sij} x_i x_j \right) = \frac{1}{n} \left(\sum_{m=1}^{n} {}^m\varepsilon_{sij} \right) x_i x_j = 0 \quad (9)$$

Equation (9) indicates that the average of the reflection positions corresponds to the reflection position of the hypothetical high-symmetry state according to Aizu (1970). The component reflections then can be indexed in accordance with the low-symmetry structure.

If the magnitude of reflection splitting is so small that it is largely masked by instrumental and other broadening contributions, the splitting might also get interpreted as line broadening of a single, unimodally broadened peak located at a position of $\varepsilon(\boldsymbol{x}) = 0$. It is reasonable to assume that in the course of a full-profile-based refinement based on such broadened diffraction data, the actual bi- or multimodal shape of the reflection splitting can reasonably be approximated by such a single unimodal peak with a variance determined by the magnitude of the reflection splitting. A bimodal delta-shaped discrete strain distribution which can be because of reflection splitting and a (unimodal) Gaussian having the same variance are illustrated in Figure 1.

It will turn out that the $\boldsymbol{x}$-dependent reflection splitting-induced line broadening because of the symmetry breaking strains ${}^m\boldsymbol{\varepsilon}_s$ is of microstrain-like character compatible with Eq. (7). The required values of $\langle \varepsilon_{ij} \varepsilon_{pq} \rangle$ can be calculated by averaging the over the strains ${}^m\boldsymbol{\varepsilon}_{sij}$ of the different domain states:

$$\langle \varepsilon_{ij} \varepsilon_{pq} \rangle = \frac{1}{n} \sum_{m=1}^{n} {}^m\varepsilon_{sij} \, {}^m\varepsilon_{spq} \quad (10)$$

Note that requirement for use of the $\langle \varepsilon_{ij} \varepsilon_{pq} \rangle$ values from Eq. (10) is validity of Eq. (1) ensuring that $\langle \varepsilon_{ij} \varepsilon_{pq} \rangle$ are truly variances and covariances (which would not be the case if Eq. (1) would not hold, i.e. $\Sigma \varepsilon_{sij} \neq 0$). The averaging resulting from Eq. (10) can easily be performed on the basis of the strain matrices for the different ferroelastic species listed by Aizu (1970). Since ${}^m\boldsymbol{\varepsilon}_s$ is invariant with respect to the symmetry operations of the low-symmetry phase's crystal class, and since the symmetry elements, which are lost in the course of symmetry reduction, act on each ${}^m\boldsymbol{\varepsilon}_s$ to form a complete set of strain tensors pertaining to all domain states, the tensor $\langle \varepsilon_{ij} \varepsilon_{pq} \rangle$ is symmetry invariant with respect to the point group (Laue class) of the high-symmetry phase. Hence, also the polynomial (7) is symmetry invariant with respect to the high-symmetry phase, as it is typically assumed to be the case (Popa, 1998; Stephens, 1999; Leineweber, 2006, 2011).

It may be interesting to analyze the direction-averaged extent of the reflection splitting-induced microstrain broadening using a measure introduced by Leineweber (2011) and a

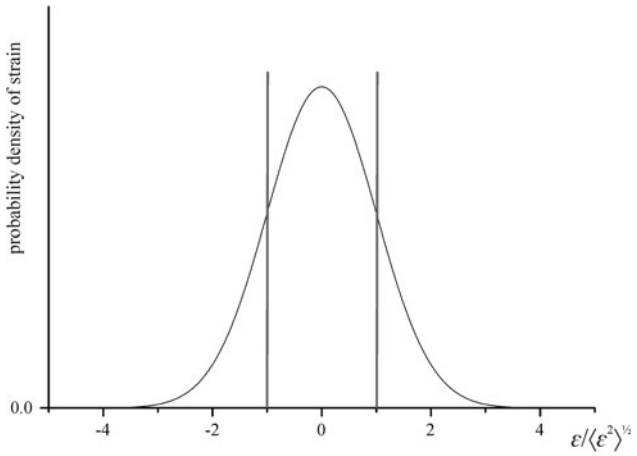

Figure 1. Probability density functions (pdfs) of a scaled strain around an average of zero and the same variances with (i) a Gaussian shape and a bimodal-delta shape represented by the two vertical lines assumed to have together the same area as the Gaussian. In a powder diffraction pattern, these pdfs may correspond to the strain distributions along the diffraction vector of a reflection *hkl* and have to be convoluted with other line broadening contributions (instrumental, size…) to yield the total measurable line profile. If these other contributions are sufficiently broad, the actual structure of the two pdfs gets masked by these, so that both pdfs will lead to a similar measurable peak profiles both located at a position corresponding to $\varepsilon = 0$.

https://doi.org/10.1017/S0885715617000665 Published online by Cambridge University Press

modified notation from Leineweber (2016). This measure amounts the direction average of $\langle\varepsilon_{hkl}^2\rangle$:

$$\overline{\langle\varepsilon_{hkl}^2\rangle} = \tfrac{1}{5}(Z_{1111} + Z_{2222} + Z_{3333} + 2Z_{1122} + 2Z_{1133} + 2Z_{2233}) \tag{11}$$

which becomes upon use of Eqs (8) and (10):

$$\overline{\langle\varepsilon_{hkl}^2\rangle} = \tfrac{1}{15n}\sum_{m=1}^{n}\left\{\begin{matrix} 3{}^m\varepsilon_{s11}^2 + 3{}^m\varepsilon_{s11}^2 + 3{}^m\varepsilon_{s11}^2 \\ +2{}^m\varepsilon_{s11}{}^m\varepsilon_{s22} + 2{}^m\varepsilon_{s11}{}^m\varepsilon_{s33} + 2{}^m\varepsilon_{s22}{}^m\varepsilon_{s33} \\ +4{}^m\varepsilon_{s12}^2 + 4{}^m\varepsilon_{s13}^2 + 4{}^m\varepsilon_{s23}^2 \end{matrix}\right\} \tag{12}$$

Addition of $0 = -({}^m\varepsilon_{s11} + {}^m\varepsilon_{s22} + {}^m\varepsilon_{s33})^2$ in the bracket yields

$$\overline{\langle\varepsilon_{hkl}^2\rangle} = \tfrac{2}{15n}\sum_{m=1}^{n}\left\{\begin{matrix} {}^m\varepsilon_{s11}^2 + {}^m\varepsilon_{s22}^2 + {}^m\varepsilon_{s33}^2 \\ +2{}^m\varepsilon_{s12}^2 + 2{}^m\varepsilon_{s13}^2 + 2{}^m\varepsilon_{s23}^2 \end{matrix}\right\} \tag{13}$$

Comparison of Eq. (13) with Eq. (6b) reveals each addend in Eq. (13) is equal, i.e. independent of m. Moreover, this comparison indicates that the

$$\overline{\langle\varepsilon_{hkl}^2\rangle} = \overline{\varepsilon^2} \tag{14}$$

holds. Hence, if microstrain broadening is induced by a slight distortion with respect to the unit cell of the high-symmetry state, the direction average of the variance of the microstrain broadening equals the direction average of the variance of the strain and is thus proportional to the squared Aizu's spontaneous strain.

IV. EXAMPLE: APPLICATION TO THE CASE TETRAGONALLY DISTORTED CUBIC MATERIALS

The case of a cubic-to-tetragonal phase transition is treated here because the line broadening associated with the corresponding reflection splitting has been considered very recently (Fabrykiewicz and Przenioslo, 2016) by describing the broadening within Stephens' (1999) description for anisotropic microstrain broadening. That description is based on the coefficients of a fourth-order polynomial in h, k, and l instead of the coefficients of the fourth-order polynomial in x_1, x_2, and x_3 as used in Eq. (7) in connection with Eq. (8), as employed here. Unfortunately, in that work, the analysis of the experimentally determined independent coefficients S_{400} and S_{220} of these polynomials remains on a qualitative basis and does not translate magnitudes of tetragonal distortion into values of S_{400} and S_{220}. This is done here within the formalism of Eqs (7) and (8), which appears to be simpler than doing so in the S_{hkl} formalism (an advantage which is even more relevant for even lower symmetries).

Assuming that the symmetry reduces from $m\bar{3}m$ to $4/mmm$ point group (corresponding to the "ferroelastic species" $m\bar{3}m$F4/mmm; Aizu, 1970), having group orders of 48 and 16, the number of domain states amounts $n = 3 = 48/16$. The strains ${}^m\boldsymbol{\varepsilon}_s$ pertaining to these domain states are:

$${}^1\boldsymbol{\varepsilon}_s = \begin{pmatrix} A & 0 & 0 \\ 0 & A & 0 \\ 0 & 0 & -2A \end{pmatrix}, \quad {}^2\boldsymbol{\varepsilon}_s = \begin{pmatrix} A & 0 & 0 \\ 0 & -2A & 0 \\ 0 & 0 & A \end{pmatrix}, \quad \text{and} \quad {}^3\boldsymbol{\varepsilon}_s = \begin{pmatrix} -2A & 0 & 0 \\ 0 & A & 0 \\ 0 & 0 & A \end{pmatrix} \tag{15}$$

Considering the distortions because of these tensors, one can calculate the distributions of strain because of the different strain states measurable in the directions $\boldsymbol{x} = (1, 0, 0)$, $\boldsymbol{x} = (1, 1, 0)/2^{1/2}$, and $\boldsymbol{x} = (1, 1, 1)/3^{1/2}$, where the occurring strains have been calculated by means of Eq. (4). The corresponding strains relative to a cubic average are shown in Figure 2 and correspond to the typical tetragonal reflection splitting in a powder diffraction pattern if this splitting is not masked by other line broadening contributions.

If that masking occurs, the coefficients of Eq. (7) describing the microstrain broadening can be calculated by use of Eqs (10) and (15) giving

$$\langle\varepsilon_{11}^2\rangle = \langle\varepsilon_{22}^2\rangle = \langle\varepsilon_{33}^2\rangle = 2A^2$$

$$\langle\varepsilon_{11}\varepsilon_{22}\rangle = \langle\varepsilon_{11}\varepsilon_{33}\rangle = \langle\varepsilon_{22}\varepsilon_{33}\rangle = -A^2$$

$$\text{and all other } \langle\varepsilon_{ij}\varepsilon_{pq}\rangle = 0 \tag{16}$$

These results indicate that the microstrain distribution is symmetry invariant with respect to the high-symmetry $m\bar{3}m$ point group.

Upon use of Eq. (16) in Eq. (7) one obtains the formula for the direction-dependent microstrain:

$$\langle\varepsilon_{hkl}^2\rangle = 2A^2\left(x_1^4 + x_2^4 + x_3^4 - x_1^2x_2^2 - x_1^2x_3^2 - x_2^2x_3^2\right) \tag{17}$$

Addition and subtraction of $+2x_1^2x_2^2 + 2x_1^2x_3^2 + 2x_2^2x_3^2$ on the right side of Eq. (17) and using $x_1^4 + x_2^4 + x_3^4 + 2x_1^2x_2^2 + 2x_1^2x_3^2 + 2x_2^2x_3^2 = 1$ yields:

$$\langle\varepsilon_{hkl}^2\rangle = 2A^2(1 - 3\Gamma) \tag{18}$$

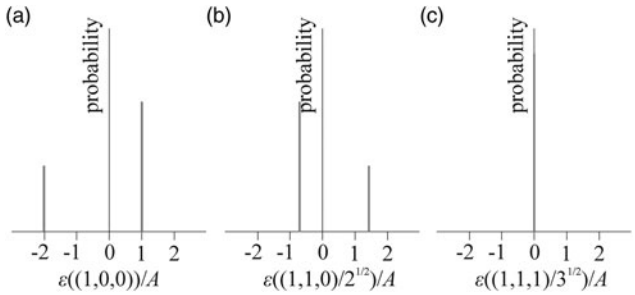

Figure 2. Distribution of strains for three different crystallographic directions for a tetragonally distorting cubic structure if all three domain states with the strains given in Eq. (15) occur with equal probability. The variances $\langle\varepsilon_{hkl}^2\rangle = \langle\varepsilon^2(\boldsymbol{x})\rangle$ of the strains according to Eq. (14) are (a) $2A^2$, (b) A^2, (c) 0 and will show up as microstrain broadening instead of reflection splitting, if the reflection splitting is sufficiently masked by other line broadening contributions.

https://doi.org/10.1017/S0885715617000665 Published online by Cambridge University Press

with $\Gamma = x_1^2x_2^2 + x_1^2x_3^2 + x_2^2x_3^2 = (h^2k^2 + h^2l^2 + k^2l^2)/(h^2 + k^2 + l^2)^2$. Thereby, the maximum value of $\langle\varepsilon_{hkl}^2\rangle$ is present for $\Gamma = 0$, i.e. $\boldsymbol{x} = (\pm1,0,0)$, $(0, \pm1,0)$, and $(0,0, \pm1)$ [Figure 2(a)] with $\langle\varepsilon_{hkl}^2\rangle = 2A^2$. This corresponds to the splitting pattern for $\{h00\}$ reflections. The minimum (zero) microstrain occurs for $\Gamma = 1/3$, i.e. $\boldsymbol{x} = (\pm1, \pm1, \pm1)$ with $\langle\varepsilon_{hkl}^2\rangle = 0$, which is the minimum possible value for a variance. This corresponds to the absent splitting of $\{hhh\}$ reflections for a symmetry reduction from cubic to tetragonal.

Note that the cubic-to-tetragonal case considered here is associated with an asymmetric distribution of the strains for all directions where the variance $\langle\varepsilon_{hkl}^2\rangle > 0$, whereas many other cases are associated with a symmetric 1:1 splitting. This direction/*hkl* dependence of this asymmetry can be considered by calculation of the third (central) moments of the microstrain distribution, on the basis of which the skewness can be calculated (Leineweber, 2009).

V. DISCUSSION

X-ray powder diffraction analysis frequently pursues to reveal the true symmetry of an investigated material. Thereby, broadening of reflections is frequently taken as a sign of a masked reflection splitting, indicative for a reduction of the crystal family with respect to that suggested by the average reflection positions. In Section III, it was shown that reflection splitting-induced line broadening, at least as it concerns the *hkl* dependence of the variance of the line broadening (here its $\boldsymbol{x}$ dependence), follows the same mathematics as "ordinary" anisotropic microstrain broadening typically employed in Rietveld refinement. This implies that identification of the correct source of line broadening can be a difficult issue, and that both options should be considered as a possibility. Hints can be obtained from the shape of the broadening, if it is sufficiently visible against the further line-broadening contributions: a mesokurtic microstrain broadening (i.e. with a shape with a top flatter than that of a Gaussian) may indicate that this broadening is indeed because of a splitting. Discernible reflection asymmetry (skewness) occurring with correct sign may also help to obtain information about a possible symmetry distortion.

The author of the present work has recently analyzed powder-diffraction data of Fe_3C (Leineweber, 2012b, 2016) and Fe_5C_2 (Leineweber *et al*., 2012). These data, could, in principle be interpreted in terms of monoclinic and triclinic symmetry, respectively, instead of in terms of the long-accepted orthorhombic and monoclinic symmetry. More detailed analysis of the diffraction data and consideration of the results from first-principles calculations implied that crystal-structure description is more adequately done in both these cases in the respective higher symmetry together with some anisotropic microstrain broadening. In these mentioned cases, the microstrain was caused by thermal microstresses because of anisotropy of the thermal expansion.

Note that reflection splitting-induced microstrain broadening can also accompany more complex symmetry reductions due superstructure formation. Detection of superstructure reflections can of course help to identify a reduction of the symmetry of the crystal family. In such case, there are always groups of domain states with the same strain (e.g. antiphase, chiral, or inversion domains). Note that the treatment here to predict reflection splitting-induced microstrain broadening considered only (ferroelastic) domain states with all different strains leading to the different ferroelastic species compiled by Aizu (1970). Cases with domain states with identical strain tensors can be treated by grouping domain states of identical strains and applying then the present formalism.

VI. CONCLUSION

The present analysis has demonstrated that the reflection splitting induced by reduction of the crystal family, which is largely masked by other line-broadening contributions, will lead to line broadening with a variance which shows a *hkl* dependence similar to that of conventional anisotropic microstrain broadening. This asks for careful consideration of both possibilities — true symmetry reduction involving reflection splitting or anisotropic microstrain broadening — to arrive at correct conclusions on the symmetry of the material under consideration.

Aizu, K. (**1970**). "Determination of the state parameters and formulation of spontaneous strain for ferroelastics," J. Phys. Soc. Japan **28**, 706–716.

Boysen, H. (**2007**). "Coherence effects in the scattering from domain structures," J. Phys.: Condens. Matter. **19**, Article No. 275206.

Carpenter, M. A., Salje, E. K. H., and Grame-Barber, A. (**1998**). "Spontaneous strain as a determinant of thermodynamic properties for phase transitions in minerals," Eur. J. Mineral. **10**, 621–691.

Cowley, J. M. and Au, A. Y. (**1978**). "Diffraction by crystals with planar faults. III. Structure analyses using microtwins," Acta Crystallogr. A **34**, 738–743.

Fabrykiewicz, P. and Przenioslo, R. (**2016**). "Distortion of the crystal structure of MnO at ambient conditions," Phys. B **489**, 56–62.

Hayward, S. A. and Salje, E. K. H. (**2005**). "Diffuse scattering from microstructures and mesostructures," Z. Kristallogr. **220**, 994–1001.

Janovec, V. and Privratska, J. (**2003**). "Chapter 3.4 domain structures," in *International Tables for Crystallography Vol. D, Physical Properties of Crystals*, edited by A. Authier (Kluwer, Dordrecht/Boston/London), pp. 449–505.

Leineweber, A. (**2006**). "Anisotropic diffraction-line broadening due to microstrain distribution; parametrization opportunities," J. Appl. Crystallogr. **39**, 509–518.

Leineweber, A. (**2009**). "Description of anisotropically microstrain-broadened line profiles by Edgeworth series," Z. Kristallogr. **224**, 432–445.

Leineweber, A. (**2011**). "Understanding anisotropic microstrain broadening in Rietveld refinement," Z. Kristallogr. **226**, 905–923.

Leineweber, A. (**2012a**). "Parabolic microstrain-like line broadening induced by random twin faulting," Philos. Mag. **92**, 1844–1864.

Leineweber, A. (**2012b**). "Anisotropic microstrain broadening in cementite, Fe_3C, caused by thermal microstress: comparison between prediction and results from diffraction-line profile analysis," J. Appl. Crystallogr. **45**, 944–949.

Leineweber, A. (**2016**). "Thermal expansion anisotropy as source for microstrain broadening of polycrystalline cementite, Fe_3C," J. Appl. Crystallogr. **49**, 1632–1644.

Leineweber, A. and Krumeich, F. (**2013**). "Broadening and shifting of Bragg reflections of nanoscale-microtwinned LT-Ni_3Sn_2," Philos. Mag. **93**, 4440–4468.

Leineweber, A., Shang, S. L., Liu, Z. K., Widenmeyer, M., and Niewa, R. (**2012**). "Crystal structure determination of Hägg carbide, χ-Fe_5C_2 by first-principles calculations and Rietveld refinement," Z. Kristallogr. **227**, 207–220.

Popa, N. C. (**1998**). "The (hkl) dependence of diffraction-line broadening caused by strain and size for all Laue groups in Rietveld refinement," J. Appl. Crystallogr. **31**, 176–180.

Stephens, P. W. (**1999**). "Phenomenological model of anisotropic peak broadening in powder diffraction," J. Appl. Crystallogr. **32**, 281–289.

https://doi.org/10.1017/S0885715617000665 Published online by Cambridge University Press